**Proceedings of ASME 2009 Conference on Smart Materials, &
Adaptive Structures and Intelligent Systems
SMASIS 2009
September 21-23, 2009, Oxnard, California, USA**

SMASIS2009-1324

DRAFT: A PHASE FIELD ANALYSIS OF THERMOMECHANICALLY COUPLED LIQUID CRYSTAL ELASTOMERS

Hongbo Wang
Florida Center for Advanced Aero-Propulsion–FCAAP
Department of Mechanical Engineering
Florida A&M/Florida State University
Tallahassee, FL 32310-6046
Email: hongbo@eng.fsu.edu

William S. Oates
Florida Center for Advanced Aero-Propulsion–FCAAP
Department of Mechanical Engineering
Florida A&M/Florida State University
Tallahassee, FL 32310-6046
Email: woates@eng.fsu.edu

ABSTRACT

A finite deformation phase field model is developed to quantify micron scale liquid crystal domain structure evolution within an elastomer network. The polymer network is described by a hyperelastic energy function and combined with a liquid crystal Landau and distortional energy function that simulates liquid crystal domain structure coupling. A theoretical framework is given which illustrates how finite deformation contributes to coupling between the liquid crystal domains and elastomer without introducing explicit phenomenological coupling constants. The model is implemented numerically using a finite element phase field approach. Domain structure evolution under thermomechanical loads are modeled to illustrate active structure responses due to the underlying liquid crystal reorientation. The model illustrates a simplified approach to predict a broad class of liquid crystal elastomer mechanics problems by implementing finite deformation within the field-coupled phase field modeling approach.

INTRODUCTION

Liquid crystal elastomers are are a fascinating class of soft actuator materials that exhibit a number of field coupled characteristics relevent to information technology, biomedical devices, and robotic systems. Liquid crystals flow like a fluid but may be oriented like a solid crystal. When these materials are synthesized within a light-weight elastomer, a number of novel material properties can be achieved such as large elastic anisotropy ($E_2/E_1 \simeq 75$) [1, 2], photomechanics [3–5], flexoelectricity [6], shape memory [7] and electrostriction [8,9]. This properties provide opportunities to design self-powered artificial organs, reversible adhesion for climbing robots [10, 11], or negative index materials for "cloaking" applications [12, 13].

Material engineering of liquid crystal elastomers requires a strong understanding of coupling between liquid crystals and the host elastomer network. Although this problem has been extensively studied [14–22], there are many open questions on the nonlinear field-coupled mechanics of these materials. A nonlinear continuum mechanics model of an elastomer network coupled with energetics of liquid crystals was presented in a previous analysis which focused on isotropic or spherical small deformation as a function of the liquid crystal orientation [23]. Here we expand this model to include finite deformation, anisotropy, and thermomechanical behavior. Coupling with finite deformation illustrates how shape changes are induced by reorientation of the liquid crystal domain structures without the need for any phenomenological parameters. Prior theoretical formulations typically introduce explicit constants between the liquid crystal order parameter and strain [24]. It is shown here that this is not necessary to predict the nonlinear constitutive behavior.

Ericksen has proposed a modeling framework for liquid crystals that includes a scalar order parameter Q and a liquid crystal director [25]. A more recent review of variational methods of liquid crystals and defect analysis can be found in [26–28]

which describes this order parameter. The scalar order parameter is a measure of anisotropy of permittivity or index of refraction. The director defines the effective orientation of the liquid crystal molecules and is constrained to be a unit vector according to the relation, $\mathbf{n}\cdot\mathbf{n}=1$ everwhere in the material body. This is combined with the scalar order parameter using the relation $Q_{ij}=Q/2(3n_in_j-\delta_{ij})$ where δ_{ij} is the Kronecker delta. This description is ill-defined when $Q\Rightarrow 0$ as observed experimentally. The director, however, is a unit vector everywhere in the material which can create strain incompatibilities [27]. Here we propose a new order parameter that avoids this issue and combines the effect of the scalar parameter Q and director n_i into a pseudo-director n_i^* that includes key features governing microscale liquid crystal domain structure evolution. The resulting model provides a phase field modeling approach that explains many of the unusual material characteristics governing this class of materials. A similar approach has been used that describes "Maxwell-like" stress in a dielectric elastomer [29, 30], except the anisotropic behavior in a liquid crystal elastomer gives rise to a number of challenging and interesting nonlinear field-coupled mechanics relations.

The outline of this paper is given as follows. A set of governing equations are presented followed by a free energy description that includes mechanical energy of the host elastomer, a Landau and distortional energy afforded by liquid crystals, and thermal effects. The model is then implemented in a nonlinear finite element phase field model to quantify domain structure evolution under large deformation and thermal loads. Several numerical examples are given to validate the theoretical model including a monodomain with a circular hole under uniaxial stretching and bending deformation under a thermal gradient. This is followed by discussion and concluding remarks in the final section.

GOVERNING EQUATIONS

A free energy function is constructed to formulate the governing equations for a nematic phase liquid crystal elastomer. The function consists of the energy components per unit current volume

$$\psi=\psi_M(F_{iK})+\psi_L(n_i^*,n_{i,j}^*) \tag{1}$$

where $\psi_L(n_i^*,n_{i,j}^*)$ is the free energy of the liquid crystal and n_i^* is an effective order parameter defining orientation of the liquid crystal mesogen units (e.g., liquid crystal forming molecule). The gradient on the liquid crystal is defined by $n_{i,j}^*$. Note that the liquid crystal director n_i^* and its gradient $n_{i,j}^*$ are both defined in the spatial configuration. The free energy of the elastomer network is denoted by $\psi_M(F_{iK})$ and F_{iK} is deformation gradient defined by [31]

$$F_{iK}=\frac{\partial x_i}{\partial X_K}. \tag{2}$$

The effective liquid crystal director order parameter is limited to the range $0\le|n_i^*|\le 1$. This is different than the traditional director n_i which is constrained to the magnitude of one everywhere in the material body. Instead, the typically used scalar parameter Q is combined with n_i to give the following second order liquid crystal tensor

$$Q_{ij}^*=\frac{1}{2}(3n_i^*n_j^*-\delta_{ij}) \tag{3}$$

which is a traceless tensor that defines uniaxial liquid crystal anisotropy in the spatial or current configuration. This tensor is proportional to the material anisotropy such as index of refraction or dielectric permittivity. This higher order tensor will be implemented in the liquid crystal energy function to quantify nematic phase behavior and coupling to the elastomer network. In the following section, we will define the liquid crystal free energy as $\psi_L=\psi_L(Q_{ij}^*,n_{i,j}^*)$. Prior to introducing this form of the energy function, the governing equation are written explicitly in terms of the order parameter n_i^* for simplification.

The free energy of liquid crystal energy is defined to be decoupled in the spatial configuration; however, coupling between the deformation gradient and liquid crystal director occurs when the energy is written in the reference configuration. This is illustrated by transforming the liquid crystal energy to the reference configuration

$$\widetilde{\psi}_L=\widetilde{\psi}_L(F_{iK},\widetilde{n}_K^*,\widetilde{n}_{K,L}^*) \tag{4}$$

where $\widetilde{n}_L^*$ and $\widetilde{n}_{K,L}^*$ are the liquid crystal director and the gradient of a liquid crystal director in the reference configuration, respectively. The relationships of the director and its gradient in reference and spatial configurations are

$$\begin{aligned} n_i^* &= J^{-1}F_{iK}\widetilde{n}_K^* \\ n_{i,j}^* &= J^{-1}F_{iK}F_{jL}\widetilde{n}_{K,L}^* \\ Q_{ij} &= J^{-1}F_{iK}F_{jL}\widetilde{Q}_{KL}^* \end{aligned} \tag{5}$$

where these relations can be obtained from virtual work principles; see [32, 33]. A rotational invariant director could have

also be obtained using the rotation tensor R_{ij} given in $\mathbf{F} = \mathbf{RU}$ where $\mathbf{U}$ is the material stretch [30], but this form is more complex. Note however that either approach yields identical field or director-coupled stresses.

The free energy function in the reference configuration is therefore denoted by

$$\widetilde{\psi} = \widetilde{\psi}_M(F_{iK}) + \widetilde{\psi}_L(F_{iK}, \widetilde{n}^*_K, \widetilde{n}^*_{K,L}). \tag{6}$$

Apply the variational method to the free energy function in the reference configuration gives

$$\begin{aligned}\delta\widetilde{\psi} &= \delta\widetilde{\psi}_M(F_{iK}) + \delta\widetilde{\psi}_L(F_{iK}, \widetilde{n}^*_K, \widetilde{n}^*_{K,L}) \\ &= \left(\frac{\partial\widetilde{\psi}_M}{\partial F_{iK}} + \frac{\partial\widetilde{\psi}_L}{\partial F_{iK}}\right)\delta F_{iK} + \left(\frac{\partial\widetilde{\psi}_L}{\partial\widetilde{n}_K}\right)\delta\widetilde{n}^*_K \\ &\quad + \left(\frac{\partial\widetilde{\psi}_L}{\partial\widetilde{n}^*_{K,L}}\right)\delta\widetilde{n}^*_{K,L}\end{aligned} \tag{7}$$

and the total energy is given by integrating (7) over the reference volume V_0

$$\begin{aligned}\delta\widetilde{\Psi} &= \int_{\Omega_0}\delta\widetilde{\psi}dV_0 \\ &= \int_{\Omega_0}\left(\frac{\partial\widetilde{\psi}_M}{\partial F_{iK}} + \frac{\partial\widetilde{\psi}_L}{\partial F_{iK}}\right)\delta F_{iK}dV_0 + \int_{\Omega_0}\frac{\partial\widetilde{\psi}_L}{\partial\widetilde{n}^*_K}\delta\widetilde{n}^*_K dV_0 \\ &\quad + \int_{\Omega_0}\frac{\partial\widetilde{\psi}_L}{\partial\widetilde{n}^*_{K,L}}\delta\widetilde{n}^*_{K,L}dV_0\end{aligned} \tag{8}$$

Use divergence theorem on the first and third terms in (8) results in a set of governing equations

$$\begin{aligned}\frac{\partial(s_{iK} + s^L_{iK})}{\partial X_K} &= 0 \\ \frac{\partial\widetilde{\xi}^*_{KL}}{\partial X_K} - \widetilde{\eta}^*_L &= 0\end{aligned} \tag{9}$$

in the reference volume subjected to a set of boundary conditions [34]. Here, s_{iK} is the nominal stress of the elastomer network and s^L_{iK} is the nominal stress contributed by liquid crystal materials. $\widetilde{\xi}^*_{KL}$ and $\widetilde{\eta}^*_L$ are the director-stress and liquid crystal director force, respectively. They are defined as

$$\begin{aligned}s_{iK} = \frac{\partial\widetilde{\psi}_M}{\partial F_{iK}}, \quad s^L_{iK} = \frac{\partial\widetilde{\psi}^L_M}{\partial F_{iK}} \\ \widetilde{\xi}^*_{KM} = \frac{\partial\widetilde{\psi}_L}{\partial\widetilde{n}^*_{K,M}} \\ \widetilde{\eta}^*_K = \frac{\partial\widetilde{\psi}_L}{\partial\widetilde{n}^*_K}\end{aligned} \tag{10}$$

The subsections below are dedicated to each component of the free energy function. In the first subsection, the neo-Hookean model is used to define mechanical energy of the host elastomer. The free energy of the liquid crystals is comprised of two parts: the Landau energy for a monodomain and Frank elastic energy for polydomain behavior. In the second and third subsections, phenomenological energy functions for different components of the liquid crystal energy are introduced and used to quantify fields and stresses in the reference and spatial configurations.

Mechanical Energy

The neo-Hookean hyperelastic energy function is introduced to quantify liquid crystal coupling to the elastomer network. This model is defined as a function of the first and third strain invariants. The principal stretches are λ_i for $i = 1,2,3$. The first and third strain invariants are $I_1 = \lambda_1^2 + \lambda_2^2 + \lambda_3^2$ and $I_3 = \lambda_1\lambda_2\lambda_3$, respectively. This function is

$$\psi_M(I_1, I_3) = \frac{\mu}{2}(I_1 - 3) - p(I_3 - 1) - \frac{p^2}{2\kappa} \tag{11}$$

where μ and κ is the shear and bulk moduli, respectively. Note that we have assumed incompressible material behavior, typical of most liquid crystal elastomers, where p serves as an indeterminate Lagrange multiplier.

The nominal stress can be obtained from

$$s^M_{iK} = 2F_{iL}\frac{\partial\psi_M}{\partial C_{KL}} \tag{12}$$

where $C_{KL} = F_{iK}F_{iL}$ [34]. Using (11), a simplified form of the nominal stress in terms of the strain invariants is

$$s^M_{iK} = \mu_M F_{iK} - pI_3F^{-T}_{iK} \tag{13}$$

see [34] for details. This hyperelastic constitutive relation is implemented in the finite element model in the following section to

quantify liquid crystal elastomer constitutive behavior for monodomain and polydomain configurations.

Landau Liquid Crystal Energy

The Landau energy component for the liquid crystal energy is defined by a truncated polynomial in terms of the second order liquid crystal tensor Q^*_{ij}. In the spatial configuration, the Landau energy is

$$\psi_L = \overline{a} Q^*_{ii} + \frac{a}{2} Q^*_{ij} Q^*_{ij} + \frac{b}{3} Q^*_{ij} Q^*_{jl} Q^*_{li} \tag{14}$$

where $\overline{a}$, a and b are phenomenological constants that define the liquid crystal phase characteristics. These terms are often temperature dependent. Thermoeffects will be considered in the later section. These coefficients are also considered to be independent of the deformation gradient. The effective molecular field in the spatial configuration is

$$\begin{aligned} \eta_i &= \frac{\partial \psi}{\partial Q^*_{kl}} \frac{\partial Q^*_{kl}}{\partial n^*_i} \\ \eta^*_i &= (\overline{a}_{KL} + a_{KLMN} Q^*_{MN} + b_{KLMNAB} Q^*_{MN} Q^*_{AB}) \times \dots \\ &\quad \frac{3}{2} (\delta_{KI} n^*_L + \delta_{LI} n^*_K) \end{aligned} \tag{15}$$

where we have introduced material parameters as functions of the deformation gradient

$$\begin{aligned} \overline{a}_{KL}(\Theta) &= F_{iK} F_{iL} \overline{a} \\ a_{KLMN}(\Theta) &= J^{-1} F_{iK} F_{jL} F_{iM} F_{jN} a \\ b_{KLMNAB} &= J^{-2} F_{iK} F_{jL} F_{jM} F_{lN} F_{lA} F_{iB} b \end{aligned} \tag{16}$$

Using the relation $\widetilde{\psi} = J\psi$ [34], $(5)_3$ and (14), the Landau energy is rewritten in the reference configuration

$$\begin{aligned} \widetilde{\psi}_{La}(F_{iK}, \widetilde{Q}^*_{KL}) = \overline{a}_{KL} \widetilde{Q}^*_{KL} + \frac{a_{KLMN}}{2} \widetilde{Q}^*_{KL} \widetilde{Q}^*_{MN} \\ + \frac{b_{KLMNAB}}{3} \widetilde{Q}^*_{KL} \widetilde{Q}^*_{MN} \widetilde{Q}^*_{AB} \end{aligned} \tag{17}$$

which gives an effective molecular field in the reference configuration

$$\begin{aligned} \tilde{\eta}_I = \frac{3}{2} \left(\overline{a}_{KL} + a_{KLMN} \widetilde{Q}^*_{MN} + b_{KLMNAB} \widetilde{Q}^*_{MN} \widetilde{Q}^*_{AB} \right) \times \dots \\ (\delta_{IK} \widetilde{n}^*_L + \delta_{LI} \widetilde{n}^*_K). \end{aligned} \tag{18}$$

The energy given by (17) has been defined such that the field in (18) is consistent with the spatial field relation given by (15). Consistency between the two fields can be shown by premultiplication of (18) by the inverse deformation gradient H_{rK}

The mechanical coupling between the liquid crystal director and elastomer network is obtained by calculating the nominal stress relation from the energy function (17) according to

$$s^{L(La)}_{iK} = \frac{\partial \tilde{\psi}_{La}}{\partial F_{iK}} \tag{19}$$

which gives

$$\begin{aligned} s^{L(La)}_{rS} = 2\overline{a} F_{rM} Q_{SM} + \frac{a}{2} J^{-1} (F_{jL} F_{rM} F_{jN} + F_{iK} F_{iM} F_{rN} \delta_{SL} \dots \\ + F_{rK} F_{jL} F_{jN} \delta_{MS} + F_{iK} F_{rL} F_{iM} \delta_{SN}) \widetilde{Q}_{KL} \widetilde{Q}_{MN} \dots \\ - \frac{a}{2} J^{-1} H_{rS} F_{iK} F_{jL} F_{iM} F_{jN} \widetilde{Q}_{KL} \widetilde{Q}_{MN} + O(3) \end{aligned} \tag{20}$$

Where the first and second order Landau effects are considered.

The Cauchy stress is then

$$\begin{aligned} \sigma^{L(La)}_{ij} = 2\overline{a} Q_{ij} + 2a Q_{ik} Q_{jk} - \frac{a}{2} Q_{mn} Q_{mn} \delta_{ij} + 2b Q^*_{im} Q^*_{ml} Q^*_{mj} \dots \\ - \frac{2b}{3} Q^*_{kl} Q^*_{ln} Q^*_{nk} \delta_{ij}. \end{aligned} \tag{21}$$

which is based on the definition $\sigma^{L(La)}_{ij} = J^{-1} F_{iK} s_{jK}$ [31].

Frank Distortion Energy

Liquid crystals often form into polydomain structures containing several regions of uniform director orientation separated by domain walls or line or point defects. During deformation, the internal liquid crystal structure may evolve from a monodomain to a polydomain state which depends on the stress, loading rate, liquid crystal phase, elastomer network, etc. Frank elastic energy [35] is introduced in this section to accommodate such domain structure evolution. Coupling to the Cauchy stress is presented here using similar arguments as presented in the previous section.

A generalized energy function for the Frank elastic energy is defined by

$$\psi_{Fr}(n^*_{i,j}) = \frac{a_{ijst}}{2} n^*_{i,j} n^*_{s,t} \tag{22}$$

in the spatial domain. The micro-stress tensor is

$$\xi^*_{ij} = \frac{\partial \psi}{\partial n^*_{i,j}} = a_{ijst} n^*_{s,t} \tag{23}$$

Note that this tensor includes both symmetric and anti-symmetric terms, $\xi^*_{ij} = \xi^s_{ij} + \xi^a_{ij}$.

A self-consistent energy relation can be written in the reference domain to illustrate coupling between the director gradient and stress. The Frank elastic energy in the reference domain is

$$\widetilde{\psi}_{Fr}(F_{iK}, \widetilde{n}^*_{K,L}) = a_{ijst} J^{-1} F_{iK} F_{jL} F_{sM} F_{tN} \widetilde{n}^*_{K,L} \widetilde{n}^*_{M,N} \tag{24}$$

The gradient field based on the reference description is given by

$$\widetilde{\xi}^*_{KL} = \frac{\partial \widetilde{\psi}}{\partial \widetilde{n}^*_{K,L}} = a_{ijst} J^{-1} F_{iK} F_{jL} F_{sM} F_{tN} \widetilde{n}^*_{M,N} \tag{25}$$

which reduces to (23) by substitution of $(5)_2$ into (25).

The stress due to a polydomain configuration is obtained similar to the monodomain liquid crystal stress by first introducing the nominal stress component. In this case, the nominal stress component due to polydomain structures is

$$\begin{aligned} s^{L(Fr)}_{rP} &= \frac{\partial \widetilde{\psi}_{Fr}}{\partial F_{rP}} \\ &= 2 a_{rjst} J^{-1} F_{jL} F_{sM} F_{tN} \widetilde{n}^*_{P,L} \widetilde{n}^*_{M,N} \\ &\quad - \frac{a_{ijst}}{2} F_{iK} F_{jL} F_{sM} F_{tN} \widetilde{n}^*_{K,L} \widetilde{n}^*_{M,N} H_{rP} \end{aligned} \tag{26}$$

and the Cauchy liquid crystal stress component is

$$\sigma^{L(Fr)}_{ji} = (a_{ilst} n^*_{j,l} + a_{list} n^*_{l,j}) n^*_{s,t} - \frac{a_{qrmn}}{2} n^*_{q,r} n^*_{m,n} \delta_{ij} \tag{27}$$

The generalized energy relation defined in (22) and liquid crystal stresses can be simplified using the typical Frank elastic energy given in the literature in terms of three phenomenological parameters [24, 35]. This energy function is

$$\begin{aligned} \psi_{Fr}(n^*_{i,j}) = &\frac{1}{2} K_1 \left(n^*_{i,i} n^*_{j,j} \right) + \frac{1}{2} K_2 \left(\in_{pjk} \in_{pst} n^*_p n^*_q n^*_{k,j} n^*_{t,s} \right) \\ &+ \frac{1}{2} K_3 \left(\in_{pmi} \in_{pjk} \in_{qmr} \in_{qst} n^*_i n^*_{k,j} n^*_r n^*_{t,s} \right) \end{aligned} \tag{28}$$

where the first term penalizes splay, the second term penalizes twist, and the third term penalizes bending of the liquid crystal director. In the single constant approximation, this energy reduces to

$$\psi_{Fr}(n_{i,j}) = \frac{1}{2} K n^*_{i,j} n^*_{i,j} \tag{29}$$

and using the single constant approximation, the fourth order tensor a_{ijkl} is related to K by

$$a_{ijkl} = K \delta_{ik} \delta_{jl} \tag{30}$$

The distortional stress is found to be symmetric in the single constant approximation by substitution of (30) into (27). This allows conventional elastic energy functions to be used to construct mechanical energy functions for stretching an elastomer network in the presence of liquid crystals without violating angular momentum relations. For more general cases, liquid crystal director forces enter the angular momentum relations which give rise to similar symmetric Cauchy stress relations on "mechanical" stresses and non-symmetric "liquid crystal" Cauchy stress components [36]. This single constant approximation will be used for numerical implementation in combination with an hyperelastic energy function given in the first subsection.

THEORY OF THERMOEFFECTS

This section is divided into two subsections. In the first subsection, the thermoeffect is introduced and coupled with the liquid crystal Landau free energy. In the next subsection, the governing equation of heat transfer are formulated.

Introduction Of Thermoeffect To Landau Energy

The phenomenological Landau parameters $\overline{a}$ and a are assumed to be functions of temperature

$$\begin{aligned} \overline{a} &= \overline{a}_0 (\Theta - \Theta_0) \\ a &= a_0 (\Theta - \Theta_0) \end{aligned} \tag{31}$$

where Θ is temperature and Θ_0 is the hypothetical phase transition temperature. By use of these expressions, the nominal stress contributed by Landau energy (20) becomes temperature dependent.

Governing Equation Of Heat Transfer

Thermal effects are introduced into the mechanical energy function

$$\begin{aligned}\psi_M(I_1,I_3,\Theta) = \frac{\mu}{2}(I_1-3) - p(I_3-1) - \frac{p^2}{2\kappa} \\ +C_v\left[(\Theta-\Theta_0) - \Theta\log\left(\frac{\Theta}{\Theta_0}\right)\right]\end{aligned} \tag{32}$$

The entropy per unit reference volume is defined by equation $\widetilde{s} = -\dfrac{\partial\tilde{\psi}}{\partial\Theta}$ [32, 34]. Note that the free energy function now consist of mechanical, thermal, and liquid crystal Landau free energy terms. The entropy change in this case is a function of temperature and the tensor Q

$$\widetilde{s} = C_v\ln\left(\frac{\Theta}{\Theta_0}\right) - \overline{a}_{KL}\widetilde{Q}^*_{KL} - \frac{a_{KLMN}}{2}\widetilde{Q}_{KL}\widetilde{Q}_{MN} \tag{33}$$

From the second law of thermodynamics

$$\Theta\dot{\widetilde{s}} \geq R - Q_{I,I} + \frac{Q_I}{\Theta}\Theta_{,I} \tag{34}$$

where Q_I is the heat flux in the reference frame and R is the heat generation rate in the volume. We define $\dot{\widetilde{s}}_g$ as entropy production to include dissipative mechanisms in addition to the thermal gradient term so that the Eqn. (34) is balanced:

$$\Theta\dot{\widetilde{s}} = R - Q_{I,I} + \frac{Q_I}{\Theta}\Theta_{,I} + \Theta\dot{\widetilde{s}}_g \tag{35}$$

By use of Duhamel's law of heat conduction [34], the caloric equation of state governing heat transfer is formulated as

$$Q_I = -Jk_{mn}H_{mI}H_{nJ}\Theta_{,J} \tag{36}$$

where k_{mn} is the spatial thermal conductivity coefficient. After substituting (36) into (35) and using (33), we have the governing equation of heat transfer

$$\begin{aligned}C_v\dot{\Theta} = R + Jk_{mn}H_{mI}H_{nJ}\Theta_{,IJ} - \frac{Jk_{mn}H_{mI}H_{nJ}\Theta_{,J}}{\Theta}\Theta_{,I} + \dots \\ 3\left(\overline{a}_{IA} + a_{IAMN}\widetilde{Q}^*_{MN}\right)\Theta\widetilde{n}^*_A\dot{\widetilde{n}}^*_I\end{aligned} \tag{37}$$

where entropy production is neglected, so $\tilde{s}_g = 0$. This illustrates that by formulating the energy balance in the reference configuration, thermal rate dependent effects on liquid crystal motion is obtained. This equation is coupled with governing equations of both liquid crystals and elastomer network in the following section.

FINITE ELEMENT IMPLEMENTATION

A nonlinear finite element approach is applied to implement the liquid crystal elastomer model. The weak form of the governing equations (9) are

$$\begin{aligned}\int_{\Omega_0} w_{i,J}(s^M_{iJ} + s^L_{iJ})dV_0 = \int_{\Gamma_0} w_i(s^M_{iJ} + s^L_{iJ})\hat{N}_J dS_0 \\ \int_{\Omega_0}\left(w_{I,J}\widetilde{\xi^*}_{JI} + w_I\widetilde{\eta^*}_I\right)dV_0 = \int_{\Gamma_0} w_I\widetilde{\xi^*}_{JI}\hat{N}_J dS_0\end{aligned} \tag{38}$$

where the weight function for mechanical equilibrium is w_i and the weight function for the liquid crystal director force balance is denoted by w_I. A unit normal in the reference configuration has been denoted by $\hat{N}_J$. Note that the nominal stress s^L_{iJ} has contributions from both Landau energy (20) and Frank energy (26).

The weak form of heat transfer equation (37) can be formulated similarly. For simplicity, we assume here that no heat source is in liquid crystal elastomers, so $R = 0$ and $\dot{\tilde{n}}^* = 0$. The liquid crystal elastomer will be in a temperature gradient field. The details of simulations will be given in the next section.

The geometry of the liquid crystal elastomer is $1 \times 1\ \mu m^2$ rectangle. In the center there is a hole whose radius is 0.06 μm. Traction and micro-stress are zero on the boundaries. The bottom is on a roller and the bottom left corner is fixed in the vertical and horizontal directions. Our simulations have shown the results are independent of mesh size, so a relatively coarse mesh is used in order to reduce computing costs. Note that this is strongly dependent on monodomain versus polydomain simulations. The parameters used in numerical implementation are given in Tab. 1. It is interesting to note that predictions of domain structures is achieved with two Landau phenomenological constants. The third order effects using b are neglected.

Table 1. PARAMETERS USED IN THE FINITE ELEMENT MODEL.

Name	Value	Unit
K	7×10^{-12}	N
$\overline{a}$	-1.5×10^5	N/m^2K
a	1×10^5	N/m^2K
b	0	N/m^2
κ	1×10^6	N/m^2
μ	2×10^5	N/m^2

NUMERICAL RESULTS

First a monodomain LCE has been considered. The initial condition is $n_1^* = 0.1$ and $n_2^* = 0$. At equilibrium pseudo-director increases to 0.94 and only points to the n_1^* direction. The simulation result is shown in Fig. 1. The anisotropic spontaneous strain predicted is 8.05% along x axis and -13.4 % along y axis, which is much larger than the one (10^{-4}) by use of infinitesimal approximation described in [23]. Further increases in spontaneous strain can be achieved by increasing the Landau parameters, but not presented here.

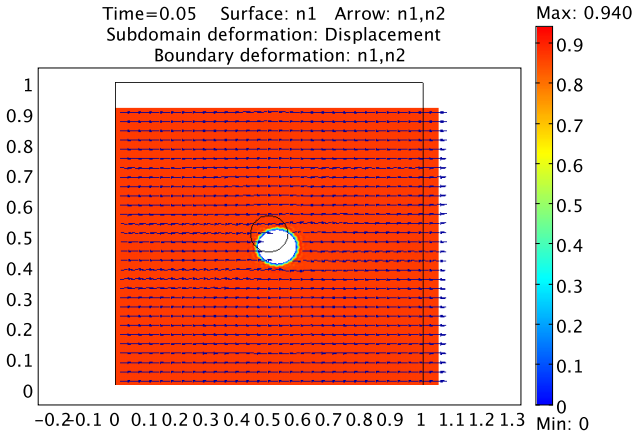

Figure 1. MONODOMAIN LIQUID CRYSTAL ELASTOMER (LCE) WITH A HOLE IN THE CENTER AT EQUILIBRIUM. THE SQUARE IS THE ORIGINAL GEOMETRY OF THE LCE FOR A ZERO PSEUDO-DIRECTOR MAGNITUDE. THE HORIZONTAL DIRECTOR COMPONENT IS SHOWN AND CORRESPONDING ARROWS.

In Figs.2 and 3, the liquid crystal polymer has been stretched along y axis. Because of coupling between liquid crystals and polymer network, the pseudo-director is reoriented along the direction of stretching. The nucleation from a monodomain and reorientation to the loading direction is illustrated in in these figures. Note that the surface plot shows the magnitude of vertical component of pseudo-director and the deformation in these figures have been scaled for visualization purposes. The stretching is approximately 300%. It is also interesting to note the corresponding stress versus stretch behavior. As shown in Fig. 4, a nonlinear constitutive response is shown that corresponds to the deformation in the previous figures. This corresponds well with soft elasticity which is a controversial subject governing this materials [24]. Here, the domain structure formation illustrates new insight on this behavior that has previously only been shown using "coarse-grain" methods [22]. The flat region on

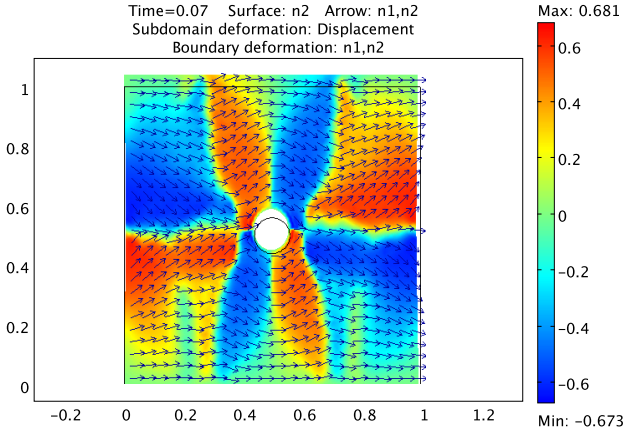

Figure 2. STRETCH OF A MONODOMAIN LIQUID CRYSTAL ELASTOMER AT 43% STRAIN.

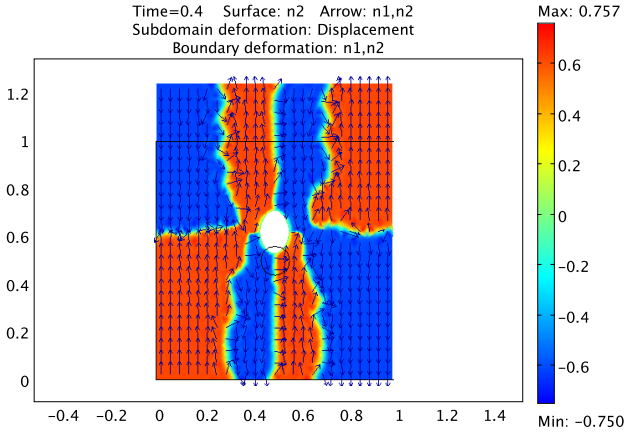

Figure 3. STRETCH OF A MONODOMAIN LIQUID CRYSTAL ELASTOMER AT 300% STRAIN.

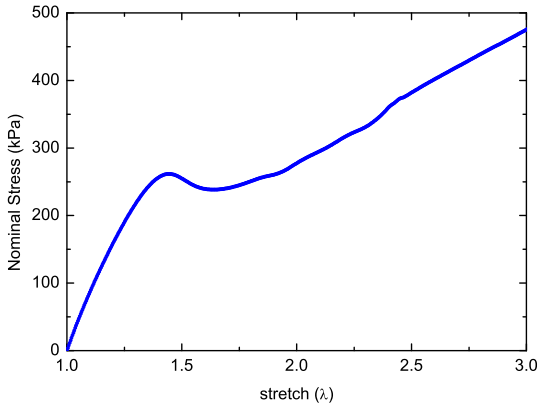

Figure 4. THE CORRESPONDING STRESS VS. STRETCH BEHAVIOR OF THE LIQUID CRYSTAL ELASTOMER WITH A CIRCULAR HOLE.

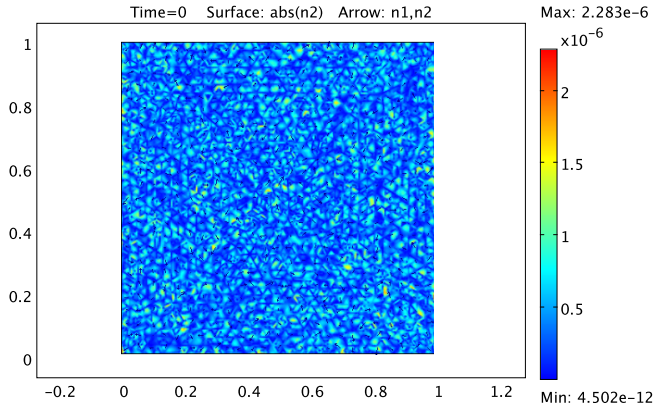

Figure 5. THE INITIAL CONDITION FOR A POLYDOMAIN LIQUID CRYSTAL ELASTOMER.

the plot is due to the reorientation of the liquid crystals with no energy penalty since they can rotate similar to a fluid, however, they provide anisotropic structure and deformation induced in the host elastomer. The circular hole is not believed to be critical in predicting this behavior since local defects are expected to be present in most compositions. Note again that this prediction is solely due to incorporation of finite deformation into the model and correct treatment of the liquid crystal pseudo-director.

In Fig. 5, the initial condition for the polydomain liquid crystal elastomer as shown. The initial conditions were created by a random number generator using Matlab. The equilibrium domain structures in spatial configuration is shown in Fig. 6. It is noted that the same order of spontaneous strains is predicted but they are not uniform on the boundaries. The domain sizes obtained are of similar to size as ones observed experimentally [24]. These results were obtained by implementing typically values for the liquid crystal energetics and hyperelastic coefficients for the elastomer network.

Lastly, we conduct simulations on a monodomain in the presence of a thermal gradient. In Fig. 7, a monodomain is simulated with the pseudo-director initially in the y (vertical) direction. A thermal gradient is introduced by applying a temperature that is larger than the isotropic liquid crystal phase transition temperature. The temperature is fixed to room temperature (below the isotropic-to-nematic) transition on the bottom of the simulation. The steady-state results of the psuedo-director reorientation and subsequent bending mode deformation is shown in Fig. 7. As expected, an isotropic phase transition occurs and results in bending deformation due to the liquid crystal reorientation. This behavior has implications on modeling photomechanical bending mode deformation of similar liquid crystal elastomers which

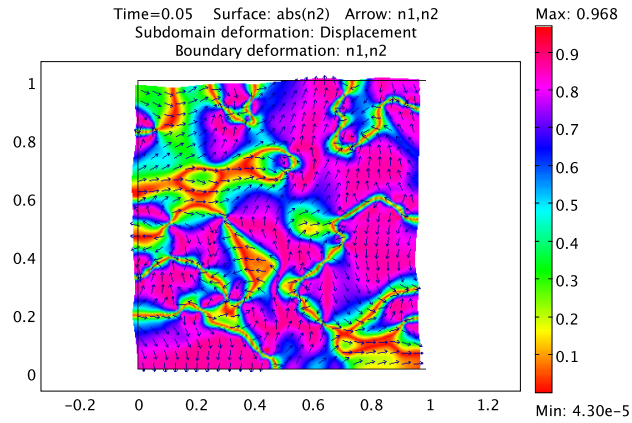

Figure 6. A POLYDOMAIN LIQUID CRYSTAL ELASTOMER AT EQUILIBRIUM.

is currently under investigation [37].

CONCLUDING REMARKS

A finite deformation model has been developed for studying the domain structure evolution in liquid crystal elastomers. The implementation of nonlinear continuum mechanics illustrates how coupling can occur between a set of liquid crystal director forces and an elastomer network without the need to introduce phenomenological coupling. This gives qualitative predictions using only two Landau parameters on spontaneous de-

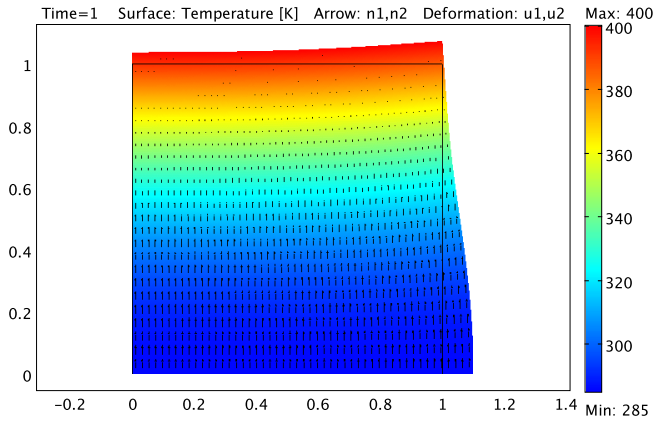

Figure 7. A MONODOMAIN LCE IN A TEMPERATURE GRADIENT FIELD. THE TEMPERATURE CONTOUR IS SHOWN ALONG WITH DEFORMATION AND THE ARROWS REPRESENTING THE LIQUID CRYSTAL ORIENTATION.

formation and liquid crystal reorientation from external thermo-mechanical loading. This also has implications on other "active" structure responses such as photo-responsive liquid crystal networks [3, 37, 38]. This behavior is currently under investigation.

ACKNOWLEDGMENT

The authors appreciate financial support by Center of Excellence, Florida Center for Advanced Aero-Propulsion- FCAAP. We also appreciate the sub-contract F5408-09-04-SC12 with General Dynamics Information Technology and discussions with T. White, T. Bunning, J. Baur, and R. Vaia at Wright Patterson Air Force Base.

REFERENCES

[1] Nishikawa, E., and Finkelmann, H., 1997. "Smectic A liquid single crystal elastomers showing macroscopic in-plane fluidity". *Macromol. Rapid Commun.,* ***18***, pp. 65–71.

[2] Acharya, B., Primak, A., and Kumar, S., 2004. "Biaxial nematic phase in bent-core thermotropic mesogens". *Phys. Rev. Lett.,* ***92***(14), pp. 145506–1–145506–4.

[3] Ikeda, T., Mamiya, J., and Yu, Y., 2007. "Photomechanics of liquid-crystalline elastomers and other polymers". *Angew. Chem.,* ***46***, pp. 506–528.

[4] Finkelmann, H., Kim, S., Muñoz, A., and Palffy-Muhoray, P., 2001. "Tunable mirroless lasing in cholesteric liquid crystalline elastomers". *Adv. Mater.,* ***13***(14), pp. 1069–1072.

[5] Palffy-Muhoray, P., Cao, W., Moreira, M., Taheri, B., and Munoz, A., 2006. "Photonics and lasing in liquid crystal materials". *Phil. Trans. Roy. Soc. A,* ***364***, pp. 2747–2761.

[6] Harden, J., Mbanga, B., Éber, N., Fodor-Csorba, K., Sprunt, S., Gleeson, J., and Jákli, A., 2006. "Giant flexoelectricity of bent-core nematic liquid crystals". *Liquid Crystal Communications*, pp. 1–11.

[7] Rousseau, I., and Mather, P., 2003. "Shape memory effect exhibited by smectic-C liquid crystalline elastomers". *J. Am. Chem. Soc.,* ***125***, pp. 15300–15301.

[8] Lehmann, W., Skupin, H., Tolksdorf, C., Gebhard, E., Zentel, R., Krüger, P., Lösche, M., and Kremer, F., 2001. "Giant lateral electrostriction in ferroelectric liquid-crystalline elastomers". *Nature,* ***410***, pp. 447–450.

[9] Spillman, C., Ratna, B., and Naciri, J., 2007. "Anisotropic actuation in electroclinic liquid crystal elastomers". *Appl. Phys. Lett.,* ***90***, pp. 021911–1–021911–3.

[10] Guduru, P., and Bull, C., 2007. "Detachment of a rigid solid from an elastic wavy surface: Experiments". *J. Mech. Phys. Solids,* ***55***, pp. 473–488.

[11] Cheng, S., and Gao, H., 2007. "Bio-inspired mechanics of reversible adhesion: Orientational-dependent adhesion strength for non-slipping adhesive contact with transversely isotropic elastic materials". *J. Mech. Phys. Solids,* ***55***, pp. 1001–1015.

[12] Harden, J., Mbanga, B., Éber, N., Fodor-Csorba, K., Sprunt, S., Gleeson, J., and Jákli, A., 2006. "Giant flexoelectricity of bent-core nematic liquid crystals". *Phys. Rev. Lett.*, pp. 157802–1–157802–4.

[13] Shalaev, V., 2007. "Optical negative-index metamaterials". *Nature Photonics,* ***1***, pp. 41–48.

[14] Martinoty, P., Stein, P., Finkelmann, H., Pleiner, H., and Brand, H., 2004. "Mechanical properties of monodomain side chain nematic elastomers". *Eur. Phys. J. E,* ***14***, pp. 311–321.

[15] Lubensky, T., Mukhopadhyay, R., Radzihovsky, L., and Xing, X., 2002. "Symmetries and elasticity of nematic gels". *Phys. Rev. E,* ***66***, pp. 011702–1–011702–22.

[16] Terentjev, E., Warner, M., and Verwey, G., 1996. "Non-uniform deformations in liquid crystalline elastomers". *J. Phys. II France,* ***6***, pp. 1049–1060.

[17] Terentjev, E., 1993. "Phenomenological theory of non-uniform nematic elastomers: Free energy of deformations and electric-field effects". *Europhys. Lett.,* ***23***(1), pp. 27–32.

[18] Warner, M., and Kutter, S., 2002. "Uniaxial and biaxial soft deformations of nematic elastomers". *Phys. Rev. E,* ***65***, pp. 051707–1–051707–9.

[19] Fried, E., and Sellers, S., 2004. "Free-energy density functions for nematic elastomers". *J. Mech. Phys. Solids,* ***52***, pp. 1671–1689.

[20] Adams, J., Conti, S., and DeSimone, A., 2007. "Soft elas-

ticity and microstructure in smectic C elastomers". *Continuum Mech. Thermodyn.,* ***18***, pp. 319–334.
[21] Adams, J., and Warner, M., 2005. "Elasticity of smectic-A elastomers". *Phys. Rev. E,* ***71***, pp. 021708–1–021708–15.
[22] Conti, S., DeSimone, A., and Dolzmann, G., 2002. "Soft elastic response of stretched sheets of nematic elastomers: a numerical study". *J. Mech. Phys. Solids,* ***50***, pp. 1431–1451.
[23] Wang, H., and Oates, W. S., 2008. "A computational modeling liquid crystal elastomers using phase field methods". *Proc. SPIE: Smart Materials and Structures*.
[24] Warner, M., and Terentjev, E., 2007. *Liquid Crystal Elastomers–Revised Edition*. Oxford Science Publications, Oxford.
[25] Ericksen, J., 1991. "Liquid crystals with variable degree of orientation". *Arch. Rational Mech. Anal.,* ***113***, pp. 97–120.
[26] Virga, E., 1994. *Variational theories for liquid crystals*. Chapman & Hall, London.
[27] Fried, E., and Sellers, S., 2006. "Incompatible strains associated with defects in nematic elastomers". *J. Chem. Phys.,* ***124***, p. 024908.
[28] Fried, E., and Todres, R., 2002. "Normal-stress differences and the detection of disclinations in nematic elastomers". *J. Polymer Sci. B: Polymer Physics,* ***40***(18), pp. 2098–2106.
[29] Zhao, X., Hong, W., and Suo, Z., 2007. "Electromechanical hysteresis and coexistent states in dielectric elastomers". *Phys. Rev. B,* ***76***, pp. 134113–1–134113–9.
[30] McMeeking, R., and Landis, C., 2005. "Electrostatic forces and stored energy for deformable dielectric materials". *J. Appl. Mech,* ***72***, pp. 581–590.
[31] Malvern, L., 1969. *Introduction to the Mechanics of a Continuous Medium*. Prentice-Hall, Inc., Englewood Cliffs, NJ.
[32] Oates, W. "A new approach to modeling liquid crystal elastomers using phase field methods". *Modelling Simul. Mater. Sci. Eng., under review*.
[33] Suo, Z., Zhao, X., and Greene, W., 2008. "A nonlinear field theory of deformable dielectrics". *J. Mech. Phys. Solids,* ***56***, pp. 467–486.
[34] Holzapfel, G., 2000. *Nonlinear Solid Mechanics*. John Wiley & Sons, Inc., Chichester.
[35] P. de Gennes, and Prost, J., 1993. *The Physics of Liquid Crystals*. Oxford Science Publications, Oxford.
[36] Wang, H., and Oates, W. "Anisotropic field-coupled mechanics of liquid crystal elastomers". *J. Mech. Phys. Solids, to be submitted*.
[37] White, T., Serak, S., Tabiryan, N., Vaia, R., and Bunning, T., 2009. "Polarization-controlled, photodriven bending in monodomain liquid crystal elastomer cantilevers". *J. Mater. Chem.,* ***19***(8), pp. 1045–1192.
[38] Harris, K., Cuypers, R., Scheibe, P., van Oosten, C., Bastiaansen, C., Lub, J., and Broer, D., 2005. "Large amplitude light-induced motion in high elastic modulus polymer actuators". *J. Mater. Chem.,* ***15***, pp. 5043–5048.